

Spin-Dependent Structure Functions in Nuclear Matter and the Polarized EMC Effect

I. C. Cloët,^{1,2,*} W. Bentz,^{3,†} and A. W. Thomas^{2,‡}

¹*Special Research Centre for the Subatomic Structure of Matter and Department of Physics and Mathematical Physics, University of Adelaide, South Australia 5005, Australia*

²*Jefferson Lab, 12000 Jefferson Avenue, Newport News, Virginia 23606, USA*

³*Department of Physics, School of Science, Tokai University, Hiratsuka-shi, Kanagawa 259-1292, Japan*
(Received 27 April 2005; published 28 July 2005)

An excellent description of both spin-independent and spin-dependent quark distributions and structure functions has been obtained with a modified Nambu—Jona-Lasinio model, which is free of unphysical thresholds for nucleon decay into quarks—hence incorporating an important aspect of confinement. We utilize this model to investigate nuclear medium modifications to structure functions and find that we are readily able to reproduce both nuclear matter saturation and the experimental F_{2N}^A/F_{2N} ratio, that is, the European Muon Collaboration (EMC) effect. Applying this framework to determine g_{1p}^A , we find that the ratio g_{1p}^A/g_{1p} differs significantly from unity, with the quenching caused by the nuclear medium being about twice that of the spin-independent case. This represents an exciting result, which, if confirmed experimentally, will reveal much about the quark structure of nuclear matter.

DOI: [10.1103/PhysRevLett.95.052302](https://doi.org/10.1103/PhysRevLett.95.052302)

PACS numbers: 25.30.Mr, 11.80.Jy, 13.60.Hb, 24.85.+p

The discovery in the early 1980s by the European Muon Collaboration (EMC) that nuclear structure functions differ substantially from those of free nucleons [1–3] caused a shock in the nuclear community. Despite many attempts to understand this effect in terms of binding corrections it has become clear that one cannot understand it without a change in the structure of the nucleon-like quark clusters in matter [4–6]. Mean-field models of nuclear structure built at the quark level, which have been developed over the past 15 years, are yielding a quantitative description of the EMC effect. Most recently it has been demonstrated that at least one of these models leads naturally to a Skyrme-type force, with parameters in agreement with those found phenomenologically to describe a vast amount of nuclear data [7].

A second major discovery by the EMC concerned the so-called “spin crisis” [8], which corresponds to the discovery that the fraction of the spin of the proton carried by its quarks is unexpectedly small. This has led to major new insights into the famous $U(1)$ axial anomaly, prompting many new experiments. With this background, it is astonishing that, in the 17 years since the discovery of the spin crisis, there has been no experimental investigation of the spin-dependent structure functions of atomic nuclei. Of course, such experiments are more difficult because the nuclear spin is usually carried by just a single nucleon and hence the spin dependence is an $\mathcal{O}(1/A)$ effect. Nevertheless, as we shall see, such measurements promise another major surprise, with at least one model—which reproduces the EMC effect in nuclear matter—suggesting a modification of the spin structure function of a bound proton in nuclear matter roughly twice as large as the change in the spin-independent structure function.

Models of nuclear structure like the quark meson coupling (QMC) model, achieve saturation through the self-

consistent change in the quark structure of the colorless, nucleon-like constituents—in particular, through its scalar polarizability [7,9]. Physically the idea is extremely simple, light quarks respond rapidly to oppose an applied scalar field. Specifically, the lower components of the valence quark wave functions are enhanced and this in turn reduces the effective σN coupling. The fact that changes in the structure of bound nucleons are so difficult to find appears to be a result of this mechanism being extremely efficient and hence yielding only a small change in the dominant upper components of the valence quark wave functions.

On the other hand, the spin structure functions are particularly sensitive to the lower components and this is why the measurement of the spin-dependent EMC effect is so promising. Our calculations are made within the framework developed by Bentz, Thomas, and collaborators [10,11], in which proper-time regularization [12–14] is applied to the Nambu—Jona-Lasinio (NJL) model in order to simulate the effects of confinement. This model exhibits similar properties to the QMC model with the advantage that it is covariant. Once we include both scalar and axial-vector diquarks, it readily describes nuclear saturation at the correct energy and density. Moreover, it yields parton distribution functions for the free nucleon [15] which are in excellent agreement with existing experimental data.

We write the spin-dependent light-cone quark distribution of a nucleus with mass number A and helicity H as the convolution

$$\Delta f_{q/A}^{(H)}(x_A) = \int dy_A \int dx \delta(x_A - y_A x) \times \Delta f_{q/N}(x) \Delta f_{N/A}^{(H)}(y_A), \quad (1)$$

where $\Delta f_{q/N}(x)$ is the spin-dependent quark light-cone

momentum distribution in the bound nucleon, $\Delta f_{N/A}^{(H)}(y_A)$ is the light-cone momentum distribution of the nucleon in the nucleus, and $x_A \in [0, A]$ is the Bjorken scaling variable for the nucleus. There have been numerous investigations of $\Delta f_{N/A}^{(H)}(y_A)$ [16] and it is straightforward to calculate for any particular nucleus. Examples of greatest experimental interest would be single proton particle or hole states like ${}^7\text{Li}$, ${}^{11}\text{B}$ and ${}^{15}\text{N}$. In this analysis, as our primary focus is the change in $\Delta f_{q/N}$ in medium, we incorporate the Fermi motion effects on the bound proton structure function by replacing $\Delta f_{N/A}^{(H)}(y_A)$ with the spin-independent distribution $f_{N/A}(y_A)$, calculated in infinite nuclear matter [11].

To calculate $\Delta f_{q/N}(x)$ in our model, it is convenient to express it in the form [17,18]

$$\Delta f_{q/N}(x) = -i \int \frac{d^4 k}{(2\pi)^4} \delta\left(z - \frac{k_-}{p_-}\right) \text{Tr}[\gamma^+ \gamma_5 M(p, k)], \quad (2)$$

where $M(p, k)$ is the quark two-point function in the nucleon. Within any model that describes the nucleon as a bound state of quarks, this distribution function can be associated with a straightforward Feynman diagram calculation, where the propagators include the self-consistent scalar and vector fields in the nucleus.

It is demonstrated in Ref. [11] that the in-medium changes to a free nucleon quark distribution can be included as follows. The effect of the scalar field is incorporated by simply replacing the free masses with the effective masses in nuclear medium, giving the distribution $\Delta f_{q/N0}(x)$, and the Fermi motion of the nucleon is included by convoluting this distribution ($\Delta f_{q/N0}(x)$) with the Fermi smearing function, $f_{N/A0}(\tilde{y}_A)$, producing the distribution

$$\Delta f_{q/A0}(\tilde{x}_A) = \int d\tilde{y}_A \int dz \delta(\tilde{x}_A - \tilde{y}_A z) \times \Delta f_{q/N0}(z) f_{N/A0}(\tilde{y}_A). \quad (3)$$

The effect of the vector field is then incorporated via the scale transformation

$$\Delta f_{q/A}(x_A) = \frac{\varepsilon_F}{E_F} \Delta f_{q/A0}\left(\tilde{x}_A = \frac{\varepsilon_F}{E_F} x_A - \frac{V_0}{E_F}\right), \quad (4)$$

where $\varepsilon_F = \sqrt{p_F^2 + M_N^2} + 3V_0 \equiv E_F + 3V_0$ is the Fermi energy of the nucleon, p_F the Fermi momentum and V_0 is the zeroth component of the vector field felt by a quark.

To calculate the spin-dependent quark distribution in the nucleon, $\Delta f_{q/N0}(x)$, we use the NJL model to describe the nucleon as a quark-diquark bound state, taking into account both scalar $J^\pi = 0^+$, $T = 0$, color $\bar{3}$ and axial-vector $J^\pi = 1^+$, $T = 1$, color $\bar{3}$ diquark channels. Details of these free space calculations, along with a description of the proper-time regularization scheme used throughout this paper, may be found in Ref. [15]. In short, the quark distribution functions are determined from the Feynman diagrams of Fig. 1, with the resulting distribution

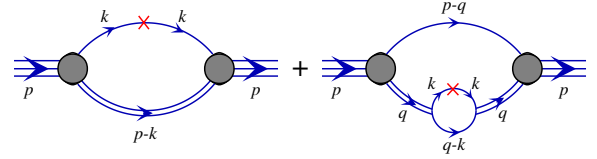


FIG. 1 (color online). Feynman diagrams representing the spin-dependent quark distributions in the nucleon, needed to determine $\Delta f_{q/N}(x)$, given in Eq. (2). The single line represents the quark propagator and the double line the diquark t matrix. The shaded oval denotes the quark-diquark vertex function and the operator insertion has the form $\gamma^+ \gamma_5 \delta(x - \frac{k_-}{p_-}) \frac{1}{2} (1 \pm \tau_z)$. The second diagram, which we refer to as the “diquark diagram,” symbolically represents two diagrams, each with the operator insertion on a different quark line within the diquark.

$\Delta f_{q/N0}(x)$, having no support for negative x . Hence, this is essentially a valence quark picture.

By calculating these Feynman diagrams using the effective (density dependent) masses obtained from the nuclear matter equation of state (discussed below) and performing the transformation, Eq. (4), to include the mean vector field, we obtain the spin-dependent u and d distributions in a bound proton. Separating the isospin factors gives

$$\Delta u_v^A(x) = \Delta f_{q/N}^s(x) + \frac{1}{2} \Delta f_{q(D)/N}^s(x) + \frac{1}{3} \Delta f_{q/N}^a(x) + \frac{5}{6} \Delta f_{q(D)/N}^a(x) + \frac{1}{2\sqrt{3}} \Delta f_{q(D)/N}^m(x), \quad (5)$$

$$\Delta d_v^A(x) = \frac{1}{2} \Delta f_{q(D)/N}^s(x) + \frac{2}{3} \Delta f_{q/N}^a(x) + \frac{1}{6} \Delta f_{q(D)/N}^a(x) - \frac{1}{2\sqrt{3}} \Delta f_{q(D)/N}^m(x). \quad (6)$$

The superscripts s , a , and m refer to the scalar, axial-vector, and mixing terms, respectively, the subscript q/N implies a quark diagram and $q(D)/N$ a diquark diagram. Because the scalar diquark has spin zero, we have $\Delta f_{q(D)/N}^s(x) = 0$ and hence the polarization of the d quark arises exclusively from the axial-vector and the mixing terms.

The NJL model is a chiral effective quark theory that is characterized by a 4-Fermi contact interaction. Using Fierz transformations any 4-Fermi interaction can be decomposed into various interacting qq and $q\bar{q}$ channels [20]. The terms relevant to this discussion are

$$\begin{aligned} \mathcal{L} = & \bar{\psi}(i\not{\partial} - m)\psi + G_\pi((\bar{\psi}\psi)^2 - (\bar{\psi}\gamma_5\vec{\tau}\psi)^2) \\ & - G_\omega(\bar{\psi}\gamma^\mu\psi)^2 + \dots \\ & + G_s(\bar{\psi}\gamma_5 C\tau_2\beta^A\bar{\psi}^T)(\psi^T C^{-1}\gamma_5\tau_2\beta^A\psi) \\ & + G_a(\bar{\psi}\gamma_\mu C\tau_i\tau_2\beta^A\bar{\psi}^T)(\psi^T C^{-1}\gamma^\mu\tau_2\tau_i\beta^A\psi), \end{aligned} \quad (7)$$

where m is the current quark mass, $\beta^A = \sqrt{\frac{3}{2}}\lambda^A$ ($A = 2, 5, 7$) are the color $\bar{3}$ matrices and $C = i\gamma_2\gamma_0$. In the $q\bar{q}$

channel we include scalar, pseudoscalar, and vector components and in the qq channel we have the scalar and axial-vector diquarks. The scalar $q\bar{q}$ interaction term generates the scalar field, that is, the constituent quark mass M (vacuum value M_0) via the gap equation. The vector $q\bar{q}$ interaction will be used to generate the vector field in-medium. The qq interaction terms give the diquark t matrices whose poles correspond to the masses of the scalar and axial-vector diquarks. The nucleon vertex function and mass, M_N , are obtained by solving the homogeneous Faddeev equation for a quark and a diquark [15]. Because we need to solve this equation many times to obtain self-consistency, we approximate the quark exchange kernel by a momentum independent form (static approximation). This necessitates the introduction of an additional parameter, c , as explained in Ref. [10].

To calculate the mean scalar and vector fields, we need the equation of state for nuclear matter. This can be rigorously derived for any NJL Lagrangian using hadronization techniques, but in a simple mean-field approximation the result for the energy density has the following form [10]:

$$\mathcal{E} = \mathcal{E}_V - \frac{V_0^2}{4G_\omega} + 4 \int \frac{d^3p}{(2\pi)^3} \Theta(p_F - |\vec{p}|) \varepsilon_p, \quad (8)$$

where $\varepsilon_p = \sqrt{\vec{p}^2 + M_N^2} + 3V_0$ and the vacuum term \mathcal{E}_V has the familiar ‘‘Mexican hat’’ shape.

The parameters of the model are Λ_{IR} , Λ_{UV} , M_0 , c , G_π , G_s , G_a , and G_ω , where Λ_{IR} and Λ_{UV} are the infrared and ultraviolet cutoffs used in the proper-time regularization. The infrared scale is expected to be of the order Λ_{QCD} and we set it to $\Lambda_{\text{IR}} = 0.28$ GeV. We also choose the free constituent quark mass to be $M_0 = 400$ MeV [21] and use this constraint to fix the static parameter, c . The remaining six parameters are fixed by requiring $f_\pi = 93$ MeV, $m_\pi = 140$ MeV, $M_N = 940$ MeV, the saturation point of nuclear matter $(\rho_B, E_B) = (0.17 \text{ fm}^{-3}, 15.7 \text{ MeV})$, and lastly the Bjorken sum rule at zero density to be satisfied, with $g_A = 1.267$. We obtain $\Lambda_{\text{UV}} = 0.66$ GeV, $c = 0.95$ GeV, $G_\pi = 17.81 \text{ GeV}^{-2}$, $G_s = 8.41 \text{ GeV}^{-2}$, $G_a = 1.36 \text{ GeV}^{-2}$, and $G_\omega = 5.58 \text{ GeV}^{-2}$.

With these model parameters the diquark masses at zero density are $M_s = 0.65$ GeV and $M_a = 1.2$ GeV and vector field strength is $V_0 = 0.044$ GeV. At saturation density the effective masses become $M^* = 0.32$ GeV, $M_s^* = 0.52$ GeV, $M_a^* = 1.1$ GeV, and $M_N^* = 0.75$ GeV.

The results for the u and d spin-dependent quark distributions, at the model scale, are presented in Fig. 2. There are four curves for each quark flavor, representing the different stages leading to the full nuclear matter result.

Using these quark distributions we are able to construct the structure functions, g_{1p} and g_{1p}^A , where the superscript A represents a structure function in the nuclear medium. Analogous results for the spin-independent quark distributions [15] allow us to determine the isoscalar structure

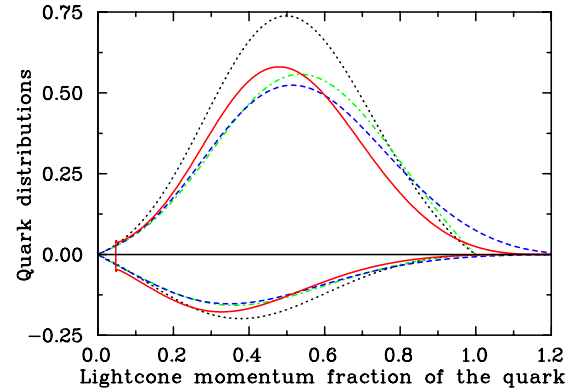


FIG. 2 (color online). Spin-dependent quark distributions, Δu_v , and Δd_v , at the model scale, $Q_0^2 = 0.16 \text{ GeV}^2$. There are four curves for each quark flavor, with the positive curves representing the up distributions. The dotted line is the free nucleon distribution, the dot-dashed line illustrates the effect of replacing the free masses with the effective ones. This distribution convoluted with the Fermi smearing function, Eq. (3), is presented as the dashed line, and the final result where the vector field is also included via the scale transformation, Eq. (4), is represented by the solid line.

functions F_{2N} and F_{2N}^A , and hence determine the EMC effect. Evolving [22] these distributions to a scale of 10 GeV^2 , we give in Fig. 3 our results for the ratios F_{2N}^A/F_{2N} and g_{1p}^A/g_{1p} , that is, the EMC and the polarized EMC effect. In the valence quark region, the model is able to reproduce the spin-independent EMC data extremely well. For the polarized ratio we find a significant effect, of the order twice the size of the unpolarized EMC effect.

The nuclear quenching effects on the individual quark flavors is presented in Fig. 4. We find that the effect on both the u and d distributions is large and approximately equal

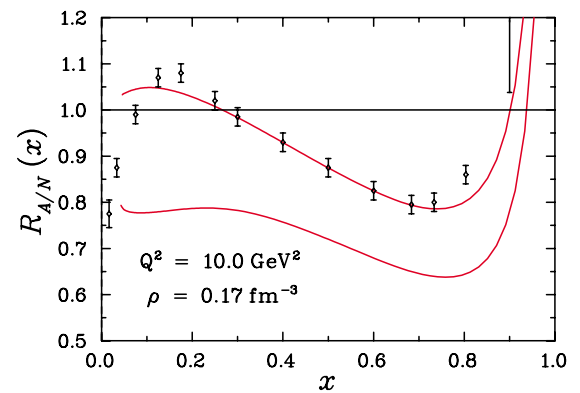


FIG. 3 (color online). Ratios of the spin-independent and spin-dependent nuclear to nucleon structure functions at nuclear matter density. The top curve is the usual EMC ratio F_{2N}^A/F_{2N} , where F_{2N} is the isoscalar structure function and the superscript A represents the in-medium result. The EMC data for nuclear matter are taken from Ref. [23]. Our prediction for the polarized EMC effect, g_{1p}^A/g_{1p} , is the lower curve.

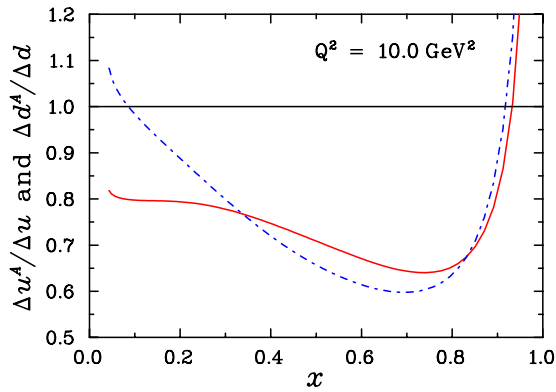


FIG. 4 (color online). Ratio of the quark distributions in nuclear matter to the corresponding free distributions, at a scale of $Q^2 = 10 \text{ GeV}^2$. The solid line represents $\Delta u^A(x)/\Delta u(x)$ and the dot-dashed line $\Delta d^A(x)/\Delta d(x)$. Note, these distributions are the full quark distributions and hence include antiquarks generated through Q^2 evolution.

over the valence quark region. The resemblance between g_{1p}^A/g_{1p} and the ratio $\Delta u^A(x)/\Delta u(x)$ is simply because the up distribution is enhanced by a factor of 4 relative to the down and strange distributions in proton structure functions. Absent from our model is the $U(1)$ axial anomaly and sea quarks (at the model scale), which prevents a reliable description of structure functions at low x . For this reason in Figs. 3 and 4 we do not plot our results in this region.

A thorough understanding of how nuclear medium effects arise from the fundamental degrees of freedom—the quarks and gluons—represents an important challenge for the nuclear physics community. An experimental measurement of the polarized EMC effect would be another important step toward this goal, providing important insights into the quark polarization degrees of freedom within a nucleus. Our prediction of a remarkably large signature suggests that this measurement is feasible, and if these results are confirmed experimentally would yield vital new information on quark dynamics in the nuclear medium.

I.C. thanks W. Melnitchouk for helpful conversations. This work was supported by the Australian Research Council and DOE contract DE-AC05-84ER40150, under which SURA operates Jefferson Lab, and by the Grant in Aid for Scientific Research of the Japanese Ministry of

Education, Culture, Sports, Science and Technology, Project No. C2-16540267.

*Electronic address: icloet@physics.adelaide.edu.au

†Electronic address: bentz@keyaki.cc.u-tokai.ac.jp

‡Electronic address: awthomas@jlab.org

- [1] J. J. Aubert *et al.* (European Muon Collaboration), Phys. Lett. B **123**, 275 (1983).
- [2] A. Bodek *et al.*, Phys. Rev. Lett. **51**, 534 (1983).
- [3] R. G. Arnold *et al.*, Phys. Rev. Lett. **52**, 727 (1984).
- [4] D. F. Geesaman, K. Saito, and A. W. Thomas, Annu. Rev. Nucl. Part. Sci. **45**, 337 (1995).
- [5] J. R. Smith and G. A. Miller, Phys. Rev. C **65**, 055206 (2002).
- [6] C. J. Benesh, T. Goldman, and G. J. Stephenson, Phys. Rev. C **68**, 045208 (2003).
- [7] P. A. M. Guichon and A. W. Thomas, Phys. Rev. Lett. **93**, 132502 (2004).
- [8] J. Ashman *et al.* (European Muon Collaboration), Phys. Lett. B **206**, 364 (1988).
- [9] G. Chanfray and M. Ericson, nucl-th/0402018.
- [10] W. Bentz and A. W. Thomas, Nucl. Phys. A **696**, 138 (2001).
- [11] H. Mineo, W. Bentz, N. Ishii, A. W. Thomas, and K. Yazaki, Nucl. Phys. A **735**, 482 (2004).
- [12] J. S. Schwinger, Phys. Rev. **82**, 664 (1951).
- [13] D. Ebert, T. Feldmann, and H. Reinhardt, Phys. Lett. B **388**, 154 (1996).
- [14] G. Hellstern, R. Alkofer, and H. Reinhardt, Nucl. Phys. A **625**, 697 (1997).
- [15] I. C. Cloët, W. Bentz, and A. W. Thomas, hep-ph/0504229.
- [16] K. Saito, M. Ueda, K. Tsushima, and A. W. Thomas, Nucl. Phys. A **705**, 119 (2002).
- [17] R. L. Jaffe, “MIT-CTP-1261 Lectures Presented at the Los Alamos School on Quark Nuclear Physics” Los Alamos, NM, 1985.
- [18] V. Barone, A. Drago, and P. G. Ratcliffe, Phys. Rep. **359**, 1 (2002).
- [19] The subscript 0 denotes the absence of any mean vector field.
- [20] N. Ishii, W. Bentz, and K. Yazaki, Nucl. Phys. A **587**, 617 (1995).
- [21] Our results do not depend strongly on this choice, remaining almost unchanged when M_0 is between 350 and 450 MeV.
- [22] M. Hirai, S. Kumano, and M. Miyama, Comput. Phys. Commun. **108**, 38 (1998).
- [23] I. Sick and D. Day, Phys. Lett. B **274**, 16 (1992).